A Novel Ordered Nanopore Array Diode Laser

V. C. Elarde, *Student Member, IEEE*, and J. J. Coleman, *Member, IEEE*

***Abstract*—In this work, we have created a new type of structure, the nanopore active layer, for achieving quantization of carrier states in a semiconductor. The nanopore structure consists of a periodic two-dimensional array of localized energy barriers perturbing an otherwise conventional quantum well. This perturbation leads to the formation of intraband forbidden energy gaps which are observed experimentally.**

***Index Terms*—Diode laser, nanopore, periodic perturbation, quantization, semiconductor laser.**

I. Introduction

THE nanopore active layer is a novel mechanism for achieving controlled quantization in a semiconductor structure. Unlike quantum dots [1]–[5], which form discrete energy levels via local confinement of carriers, the nanopore structure achieves quantization in a distributed fashion, via resonant scattering of electrons. The result is the introduction of forbidden energy bands into the conduction and valence bands of the semiconductor. This effect is similar to the formation of the bands of a bulk semiconductor resulting from the periodic potential structure of the atomic crystal lattice. A schematic illustration of the nanopore active layer is included as Fig. 1.

We have previously reported on the fabrication of patterned quantum-dot lasers using direct-write electron beam lithography and selective area epitaxial regrowth by metal–organic chemical vapor deposition (MOCVD) [6]–[8]. In this work, we have extended this fabrication process to create semiconductor laser diodes containing a nanopore active layer. Computational simulation of the mechanism for achieving distributed quantization and experimental demonstration of the nanopore effect are presented.

II. Theory of the Nanopore Laser

The energy states of a quantum well are typically modeled using a one-dimensional, finite barrier, particle-in-a-box along the direction perpendicular to the plane of the quantum well. In the plane of the well, the free-electron model is used in which a parabolic relationship exists between the electron's in-plane momentum wavevector and its energy.

The nanopore active layer is modeled using the same one-dimensional particle-in-a-box model for the perpendicular direction; however, the in-plane structure requires additional considerations. The two-dimensional in-plane structure of the nanopore is modeled as a low-energy background perturbed in a periodic manner by circular, higher-energy, barrier regions. These barrier regions are arranged on a hexagonal lattice.

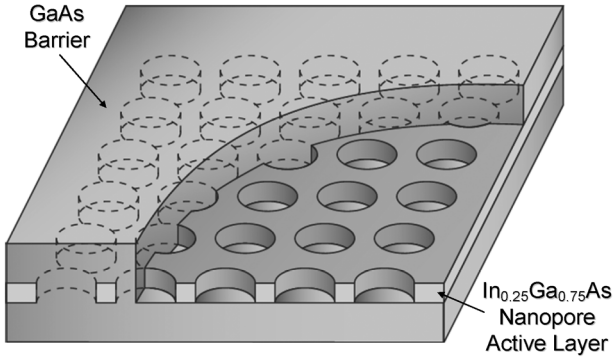

Fig. 1. Schematic illustration of the nanopore active layer which consists of an array of GaAs barrier regions perturbing an InGaAs quantum well.

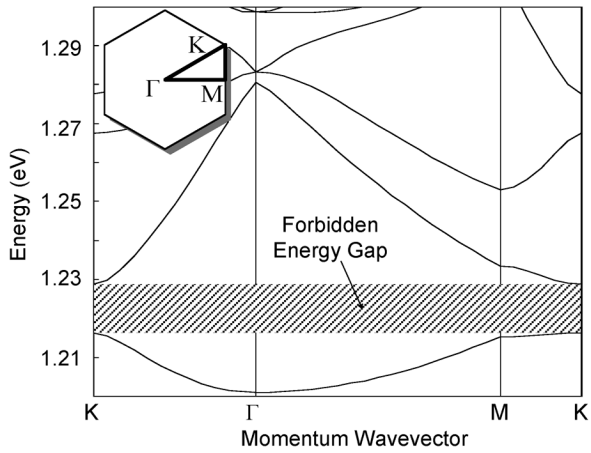

Fig. 2. Calculated dispersion relation for the couduction band of a nanopore structure containing 10-nm diameter barrier regions arranged on a hexagonal lattice with a center-to-center spacing of 20 nm. The forbidden energy gap created by the periodic structure has been indicated. A similar dispersion relation with a smaller forbidden energy gap (due to the increased effective mass of holes) has been calculated for the valence band. Inset: Illustration of the first Brillouin zone with bounding points labeled.

The energy structure of the nanopore layer is calculated using a numerical method, namely the finite-difference method, applied to a single unit cell of the periodic array. Periodic boundary conditions are necessarily used as the wavefunctions corresponding to the solutions are highly distributed for this structure. Interactions between neighboring unit cells, therefore, cannot be neglected as is often done for the case of quantum dots. This system is solved to find the dispersion relation over the first Brillouin zone for the nanopore structure. The conduction band dispersion relation is presented in Fig. 2. The periodically arranged barriers result in the formation of an intraband, forbidden energy gap as has been indicated in the figure. The forbidden energy band forms as a result of resonant

Manuscript received May 25, 2007; revised October 21, 2007. This work was supported in part by the Defense Advanced Research Projects Agency (DARPA) under Grant 433143-874a and in part by the National Science Foundation under Grant 03-35082.

The authors are with the Department of Electrical and Computer Engineering, University of Illinois, Urbana-Champaign, IL 61801 USA (e-mail: vcelarde@uiuc.edu).

Digital Object Identifier 10.1109/LPT.2007.912978

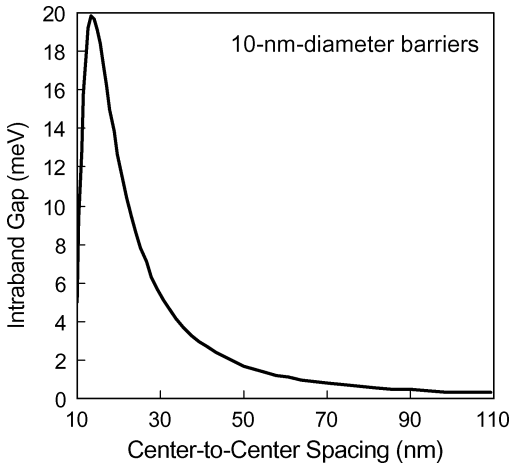

Fig. 3. Plot of the size of the intraband gap created in the conduction band by the nanopore structure corresponding to 10-nm-diameter barrier regions on a hexagonal lattice with varying center-to-center spacing.

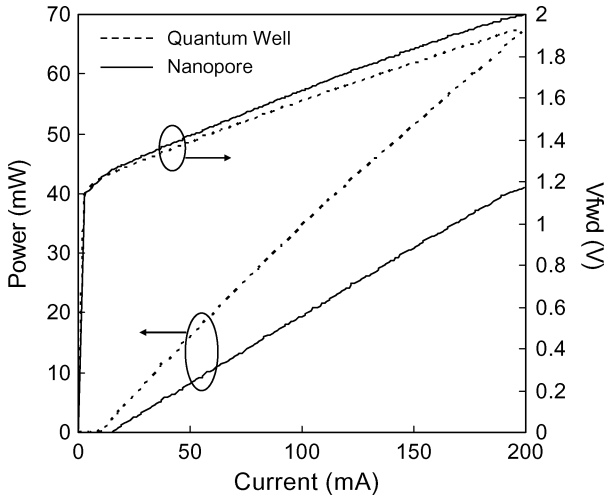

Fig. 4. Light and voltage versus current data for the nanopore laser diodes and the quantum-well control devices taken at room temperature. The quantum efficiency of the nanopore lasers is reduced from that of the quantum-well devices as a result of damage induced by the electron beam lithography.

scattering of electrons by the periodically arranged barrier regions. Conceptually, this effect is similar to the formation of the photonic bandgap in a photonic crystal through resonant scattering of photons by the periodic index of refraction structure.

Through manipulation of the nanopore geometry, the size of the intraband energy gap can be controlled and, therefore, designed for a particular application. The size of the induced intraband gap in the conduction band for a nanopore array consisting of 10-nm-diameter barrier regions on a varying pitch is plotted in Fig. 3, to illustrate the design freedom that is possible.

III. Fabrication of Nanopore Laser Diodes

Initially, a base structure is grown on an n-type GaAs wafer which consists of a 1-μm-thick layer of n-type $Al_{0.75}Ga_{0.25}As$, which acts as the lower cladding, and a 100-nm-thick intrinsic layer of GaAs, which forms the lower barrier. This and all subsequent growth steps are carried out at atmosphereic pressure in a Thomas Swan MOCVD reactor using TMG, TMI, TMA, and arsine gas as sources. Hydrogen silsesquioxane (HSQ) is then spun on the wafer and electron-beam lithography is performed in a JEOL JBX-6000 series electron beam lithography tool. The pattern consists of an array of points on a hexagonal lattice with 80-nm center-to-center spacings. The HSQ becomes silicon dioxide in the areas where it was written which will act as the selective area growth mask in the subsequent regrowth step. The unwritten HSQ is developed away using a solution of tetra-methyl-ammonium-hydroxide (TMAH). This leaves an array of silicon dioxide dots of approximately 40-nm diameter on the surface. The sample is then returned to the reactor for the growth of an 8-nm-thick layer of $In_{0.25}Ga_{0.75}As$ and a 10-nm-thick GaAs cap, which forms the nanopore active layer in patterned regions and an ordinary quantum well elsewhere.

The silicon dioxide growth mask is then removed using buffered hydrofluoric acid solution and the sample is returned to the reactor for the growth of the upper barrier. This regrowth consists of a 90-nm-thick layer of intrinsic GaAs. Next, 4-μm-wide ridges are etched over the nanopore regions to act as a lateral waveguide for the completed devices. The etch is performed using $1 : 8 : 80 H_2SO_4 : H_2O_2 : H_2O$, and is approximately 125-nm deep. This depth was determined to be optimal to form a single-lateral-mode waveguide and also sufficiently deep to remove the quantum-well region immediately surrounding the nanopore region to avoid carrier diffusion into that region during device operation. Finally, a third regrowth step is performed which consists of a 10-nm-thick layer of intrinsic GaAs to complete the upper barrier, a 1-μm-thick layer of p-type $Al_{0.75}Ga_{0.25}As$ to provide the upper cladding, and a 100-nm-thick, GaAs p+ contact layer.

A 1000-Å-thick layer of SiO_2 is then deposited by plasma-enhanced chemical vapor deposition and 3-μm-wide stripes are etched above the buried ridges to form a current aperture. Top-side contact metals are then deposited which consist of Ti, Pt, and Au. The sample is then thinned to $\sim$100 μm to facilitate cleaving. Finally, back-side metals are deposited, consisting of Ge : Au, Ni, and Au. The sample is then diced into individual devices with 1-mm cavity lengths. In addition to the devices containing a nanopore active layer, devices from unpatterned regions of the sample are fabricated as well. These devices contain an ordinary quantum-well active layer and are used as control devices for comparison to the nanopore lasers.

IV. Nanopore Laser Results

Both nanopore lasers and quantum-well lasers were tested under pulsed current injection at room temperature using 2-μs pulsewidths with a 0.3% duty cycle. The light versus current and voltage versus current data for both device types taken at room temperature are presented in Fig. 4. The slope efficiency of the nanopore devices is slightly lower than that of the quantum-well devices. We believe this is due to damage to the crystal structure caused by the electron beam lithography. We have noticed a similar, although less substantial, decrease in quantum efficiency for patterned quantum-dot devices in previous work which we believe to be caused by the same effect. The more dramatic reduction in quantum efficiency observed in the nanopore devices is consistent with the higher dose required for HSQ exposure (used for the nanopore process) than for PMMA exposure (used for the patterned quantum dots).

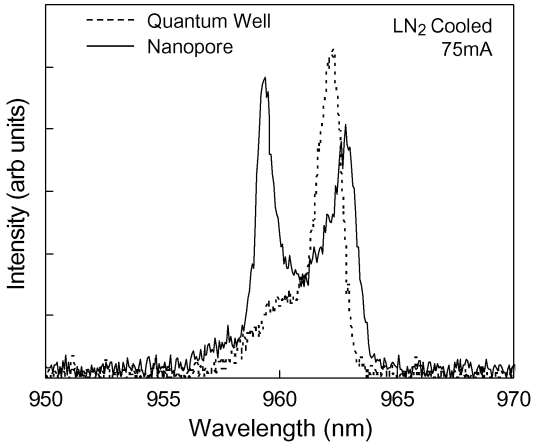

Fig. 5. Spectra from a quantum well and a nanopore laser device taken under identical injection conditions near 77 K. The nanopore laser spectrum contains two distinct lasing peaks, indicative of the presence of a forbidden energy gap.

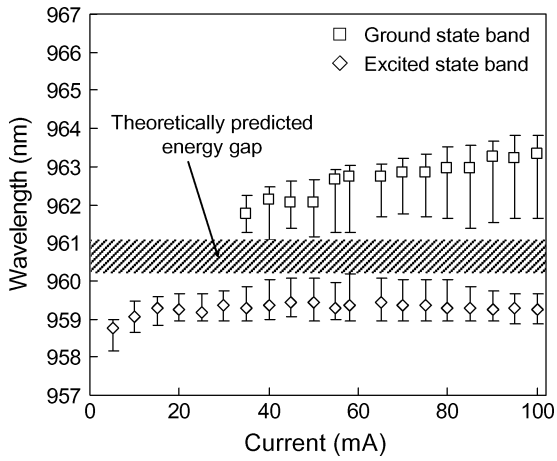

Fig. 6. Plot of the peak wavelengths for the ground state band and excited state band emission from a nanopore laser device. The vertical bars in the figure indicate the full-width at half-maximum of each peak. The shaded horizontal band indicates the theoretically predicted width of the forbidden energy gap.

A series of spectra corresponding to a range of injection currents was taken from both the nanopore and quantum-well devices in an evacuated chamber on a liquid nitrogen cooled stage. The nanopore devices exhibited a distinct, dual-peaked spectrum over a large range of injection currents, which we believe is indicative of the presence of an intraband forbidden energy gap. The two peaks correspond to emission from both the ground state and excited state emission bands. A comparison of the nanopore and quantum-well emission spectra under identical injection conditions is presented in Fig. 5. The ground state band emission of the nanopore laser is also slightly red-shifted compared to the emission from the quantum well device. This is likely due to a small amount of growth rate enhancement in the patterned regions during the regrowth of the active layer due to the reduced surface area. This results in a slightly thicker active layer for the nanopore devices compared to the quantum-well devices and a corresponding red shift of the emission spectrum.

Fig. 6 contains a plot of the peak emission wavelength for the ground state and excited state emission bands of the nanopore laser as a function of current. The vertical bars in the figure indicate the full-width at half-maximum of the peak.

The excited state emission peak remains fairly constant both in wavelength and width over the entire range of injection currents. The ground state emission broadens with increased injection which may be a result of gain-saturation effects. The emission stop band is present over the entire range of injection currents and has a width of just under 1 nm which is in approximate agreement with the size of the intraband forbidden energy gap for this structure expected from simulations. The width of the predicted stop band has been indicated in Fig. 6 by the shaded band.

V. Conclusion

We have developed a novel structure, the nanopore active layer, for achieving artificially induced quantization of carriers in a semiconductor device. This structure consists of a periodically perturbed quantum well containing higher-energy barrier regions on an ordered hexagonal lattice. We have predicted the formation of an intraband forbidden energy gap resulting from resonant scattering of electrons by this structure. Laser diodes based on the nanopore active layer have been fabricated and have been used to experimentally demonstrate the presence of the forbidden energy gap via observation of the laser spectra.

References

[1] O. B. Shchekin, P. Gyoungwon, D. L. Huffaker, and D. G. Deppe, "Discrete energy level separation and the threshold temperature dependence of quantum dot lasers," *Appl. Phys. Lett.*, vol. 77, no. 4, pp. 466–468, Jul. 24, 2000.

[2] P. Blood, "On the dimensionality of optical absorption, gain, and recombination in quantum-confined structures," *IEEE J. Quantum Electron.*, vol. 36, no. 3, pp. 354–362, Mar. 2000.

[3] P. Blood, "Quantum dot laser diodes: Physics, progress and potential," in *Conf. Lasers Electro-Optics (CLEO)*, May 19–24, 2002, vol. 1, pp. 555–556.

[4] Y. Ning, X. Gao, L. Wang, P. Smowton, and P. Blood, "Lasing characteristics of coupled InGaAs/GaAs multi-layers quantum dots laser," in *Proc. 6th Int. Conf. Solid-State Integrated-Circuit Technology*, Oct. 22–25, 2001, vol. 2, pp. 1249–1251.

[5] N. N. Ledentsov, D. Bimberg, V. M. Ustinov, Z. I. Alferov, and J. A. Lott, "Self-organized InGaAs quantum dots for advanced applications in optoelectronics," in *IEEE Int. Conf. Indium Phosphide Related Materials (IPRM 2001)*, May 14–18, 2001, pp. 5–8.

[6] V. C. Elarde and J. J. Coleman, "Spectral and threshold performance of patterned quantum dot lasers," *Phys. Stat. Sol. (c)*, vol. 3, pp. 508–511, 2006.

[7] V. C. Elarde, A. C. Bryce, and J. J. Coleman, "High performance laser with nanopatterned active layer by selective area epitaxy," *Electron. Lett.*, vol. 41, no. 20, pp. 1122–1124, Sep. 2005.

[8] V. C. Elarde, T. S. Yeoh, R. Rangarajan, and J. J. Coleman, "Controlled fabrication of InGaAs quantum dots by selective area epitaxy MOCVD growth," *J. Cryst. Growth*, vol. 272, pp. 148–153, 2004.